Quantum Monte Carlo study of a one-dimensional phase-fluctuating condensate in a harmonic trap

C. Gils,[1] L. Pollet,[1] A. Vernier,[2] F. Hebert,[2] G.G. Batrouni,[2] and M. Troyer[1]
[1]*Institut für Theoretische Physik, ETH Zürich, CH-8093 Zürich, Switzerland*
[2]*Institute Non-Linéaire de Nice, UMR CNRS 6618, Université de Nice-Sophia Antipolis, 1361 route des Lucioles, F-06560 Valbonne, France*

(Dated: February 6, 2008)

We study numerically the low-temperature behavior of a one-dimensional Bose gas trapped in an optical lattice. For a sufficient number of particles and weak repulsive interactions, we find a clear regime of temperatures where density fluctuations are negligible but phase fluctuations are considerable, i.e. , a quasicondensate. In the weakly interacting limit, our results are in very good agreement with those obtained using a mean-field approximation. In coupling regimes beyond the validity of mean-field approaches, a phase-fluctuating condensate also appears, but the phase-correlation properties are qualitatively different. It is shown that quantum depletion plays an important role.

PACS numbers: 03.75.Hh, 03.75.Lm,05.30.Jp

In a spatially homogeneous one-dimensional (1D) gas of bosons, spontaneous symmetry breaking is excluded at all temperatures T [1, 2, 3]. Long-range order is absent in this system due to the fluctuations of the phase of the order parameter, as seen in the asymptotic decay of the equal-time single-particle Green's function (algebraic for $T = 0$ and exponential for $T > 0$) [4, 5, 6, 7]. However, analytical studies of trapped 1D bose gases with a fixed particle number, N, reveal new phenomena. For example, the ground state of a noninteracting 1D bose gas in a harmonic trap with frequency ω becomes macroscopically populated below a temperature $T_c \simeq N\hbar\omega/\ln(2N)$, i.e. , a Bose-Einstein condensate (BEC) exists in the finite system [8]. Several mean-field studies indicate that weak repulsive interactions introduce an additional effect, namely, that fluctuations of the density are suppressed at low temperatures, and a phase-fluctuating condensate, or quasicondensate, appears [9, 10, 11, 12, 13, 14]; for the homogeneous system see [15]. Roughly speaking, this is a regime in temperature where the distribution of particles in space is given by a temperature-independent Thomas-Fermi profile, while thermal fluctuations of the phase are present and lead to a phase-coherence length that is smaller than the condensate cloud. Only below a much lower temperature do phase fluctuations also become negligible and phase coherence extends over the complete condensate cloud. A phase-fluctuating condensate emerges only in low dimensions and has been experimentally observed in sufficiently anisotropic 3D trapping geometries [16].

In this paper, we verify the existence of a 1D quasicondensate, on trapped optical lattices, starting from a microscopic approach whose validity is not restricted to certain parameter regimes. Using quantum-Monte Carlo simulations of the Bose-Hubbard model, we investigate the properties of the phase-fluctuating condensate for various choices of interaction strength and density. For weak interactions, our results are in excellent agreement with mean-field estimates in the continuum [10]. In an intermediate-coupling regime beyond the weakly interacting limit, but not yet in the strong-coupling domain, the quasicondensate regime spreads over an even larger temperature range. Nonetheless, we observe qualitatively different phase-correlation properties which do not follow from existing analytical approaches.

First, we briefly review the notion of a quasicondensate (QC) in a weakly interacting (WI) 1D trapped bose gas as presented in [10]. In the WI limit, we have $\gamma = mg/\hbar^2 n \ll 1$, where n is the average particle density, m the particle mass, and g the coupling constant of a repulsive contact interaction [17]. In second-quantized representation, the Hamiltonian of the system is given by

$$\hat{H} = \int dz\, \hat{\psi}^\dagger(z) \left(-\frac{\hbar^2\nabla^2}{2m} + V_{\rm t}(z) + \frac{g}{2}\hat{\psi}^\dagger(z)\hat{\psi}(z) \right) \hat{\psi}(z), \tag{1}$$

where $\hat{\psi}(z)$ is the bosonic field operator and $V_{\rm t}(z) = m\omega^2 z^2/2$ the external trapping potential centered at the origin. The authors in [10] show that density fluctuations $\langle \delta\hat{n}(z)\delta\hat{n}(z')\rangle$, where $\hat{n}(z) = n(z) + \delta\hat{n}(z)$, are suppressed for inverse temperatures $\beta \gg \beta_d = (N\hbar\omega)^{-1}$ (Boltzmann constant $k_B = 1$). The field operator can then be expressed as $\hat{\psi}(z) = \sqrt{n(z)}\exp[i\hat{\phi}(z)]$. Thermal fluctuations of the phase are evident from the decay of the one-particle density matrix, or (equal-time) Green's function, which is obtained as [10]

$$\langle \hat{\psi}^\dagger(z)\hat{\psi}(z')\rangle = \sqrt{n(z)n(z')}\exp(-\langle\delta\hat{\phi}^2_{zz'}\rangle/2), \tag{2a}$$

where $\delta\hat{\phi}^2_{zz'} = (\hat{\phi}(z) - \hat{\phi}(z'))^2$, and

$$\langle\delta\hat{\phi}^2_{zz'}\rangle = \frac{4\beta_d\mu_{\rm TF}}{3\beta\hbar\omega}\left|\ln\left(\frac{(L_{\rm TF}-z')}{(L_{\rm TF}+z')}\frac{(L_{\rm TF}+z)}{(L_{\rm TF}-z)}\right)\right|, \tag{2b}$$

where $\mu_{\rm TF} = (3Ng/4)^{2/3}(m\omega^2/2)^{1/3}$ is the chemical potential, and $L_{\rm TF} = \sqrt{2\mu_{\rm TF}/m\omega^2}$ the half size of the

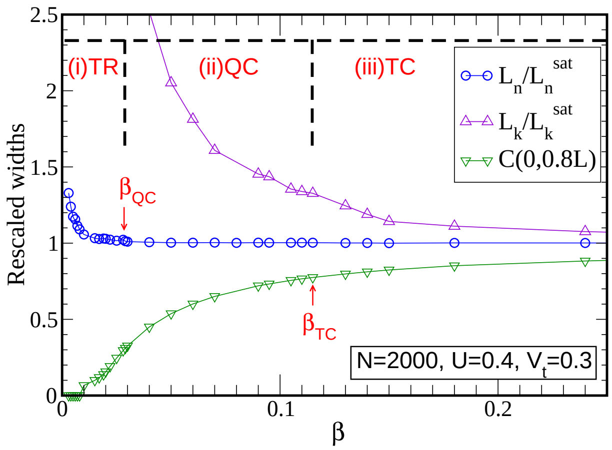

FIG. 1: (Color online)(i) Thermal regime: As a result of both density and phase fluctuations, the widths of the density profile, L_n, and the momentum profile, L_k, depend on β with $L_n(\beta) > L_n^{\rm sat}$, $L_k(\beta) > L_k^{\rm sat}$. (ii) Quasicondensate: Density fluctuations are negligible ($L_n = L_n^{\rm sat}$, L is the half size of the condensate cloud for $\beta \geq \beta_{\rm QC}$). However, the phase fluctuates, as seen for $L_k(\beta) > L_k^{\rm sat}$, phase correlation function $C(0, 0.8L) < 1$. (iii) True condensate: Phase fluctuations also disappear as $L_k(\beta)$ approaches $L_k^{\rm sat}$, and $C(0, 0.8L)$ approaches 1. The numerical results are $\beta_{\rm QC} \approx 0.03$ and $\beta_{\rm TC} = 0.115(5)$ (analytical estimate: $\tilde{\beta}_{\rm TC} = 0.116$).

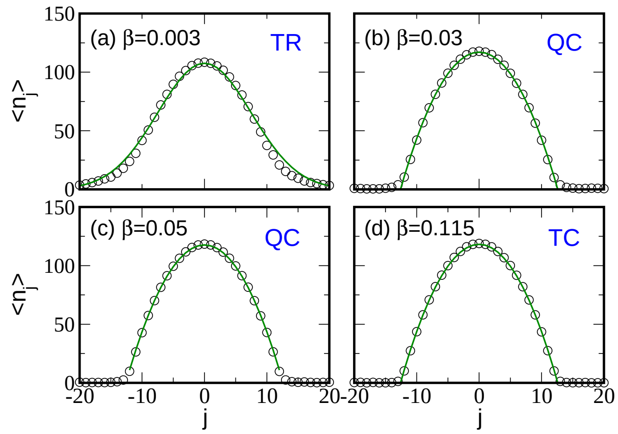

FIG. 2: (Color online) $N = 2000$, $U = 0.4$, $V_t = 0.3$ ($\gamma = 0.003$). Density fluctuations are suppressed for $\beta \geq \beta_{\rm QC} \approx 0.03$ and the density profiles $n_j = \langle \hat{n}_j \rangle$ ($\circ$) are identical for $\beta \geq \beta_{\rm QC}$ (b)-(d). In (a), the line is a fit to a Gaussian profile, while in (b)-(d) the lines are fits to a TF profile $n_0(1 - j^2/L^2)$ where $L = 12.6$ ($L_{\rm TF} = 12.6$). Error bars in the figures are always smaller than the symbol size.

condensate in the Thomas-Fermi (TF) approximation ($\mu_{\rm TF} \gg \hbar\omega$; see e.g. [19]). For $\beta \to \infty$, it follows from Eq. (2b) that $\langle \delta\hat{\phi}_{zz'}^2 \rangle \to 0$, and thus $G(z, z') \to \sqrt{n(z)n(z')}$, i.e. the system is completely phase coherent.

As is well known [18], the discretization of Eq. (1) yields the Bose-Hubbard model with lattice Hamiltonian

$$\hat{H} = -J \sum_{\langle j,j' \rangle} (\hat{a}_j^\dagger \hat{a}_{j'} + {\rm H.c}) + \frac{U}{2} \sum_j \hat{n}_j(\hat{n}_j - 1) + V_t \sum_j (j - M/2)^2 \hat{n}_j, \quad (3)$$

where $\hat{a}_j^\dagger$ creates a particle at optical lattice site j and $\hat{n}_j = \hat{a}_j^\dagger \hat{a}_j$. The number of lattice sites M is chosen such that the occupation at the boundaries of the lattice is zero. We work in units where the lattice spacing and $\hbar^2/2m$ are set to 1. In these units, parameters in Eqs. (1) and (3) are related as follows: $J = 1$, $U = g$, $V_{\rm t} = (\hbar\omega)^2/4$. Our system is defined on an optical lattice, however, in the WI and degenerate limits, the discrete and continuum description of the phase-fluctuating condensate are equivalent [12]. We investigate this model using a worm update quantum Monte Carlo (QMC) method in the canonical ensemble [20]. This nonlocal update scheme allows for an efficient evaluation of the equal-time Green's function $G(j, j') = \langle \hat{a}_j^\dagger \hat{a}_{j'} \rangle$. Phase correlation properties are also apparent from the shapes of the momentum profile, $n(k) = \sum_{j,j'} G(j, j') \exp[ik(j - j')]$, and the rescaled Green's function (phase correlation function), $C(j, j') = G(j, j')/\sqrt{n_j n_{j'}}$, where $n_j = \langle \hat{n}_j \rangle$ is the density distribution. In the WI, TF and mean-field (N large enough) limits, we observe three different regimes in temperature: the thermal regime (TR), the quasicondensate (QC) and the "true condensate" (TC). These regimes are separated by smooth crossovers, which are characterized by the temperatures $1/\beta_{\rm QC}$ and $1/\beta_{\rm TC}$. We discuss the properties of the three regimes and compare our results with the mean-field results listed above. Furthermore, we consider the emergence of the phase-fluctuating condensate depending on the choice of parameters N, U and V_t, including parameter sets that are beyond the WI limit.

In the thermal regime $\beta < \beta_{\rm QC}$, both the density and the phase are governed by thermal fluctuations. Hence, all quantities exhibit a strong temperature dependance. The width of the density profile, $L_n(\beta)$ (standard deviation of n_j), decreases throughout the TR, until it reaches its minimum value $L_n^{\rm sat}$ at the inverse temperature $\beta_{\rm QC}$, as shown in Fig. 1. The shape of the density profile is approximately Gaussian, which is expected for high temperatures where the bosonic nature of the particles becomes less relevant [Fig. 2 (a)]. The strong phase fluctuations are seen in the width of the momentum profile, $L_k(\beta)$ [standard deviation of $n(k)$], which is much larger than its minimum value $L_k^{\rm sat}$ [Fig. 1], as well as in the exponential decay of the Green's function [Fig. 3 (a)]. We recall that there exists no analytical estimate for $\beta_{\rm QC}$; density fluctutations are merely predicted to become small for $\beta \gg \beta_d = (4V_t N^2)^{-1/2}$ [10]. For the parameter set in the Figs. 1-3 , we have $\beta_d \approx 0.02\beta_{\rm QC}$.

In the quasicondensate ($\beta_{\rm QC} \leq \beta < \beta_{\rm TC}$), the density

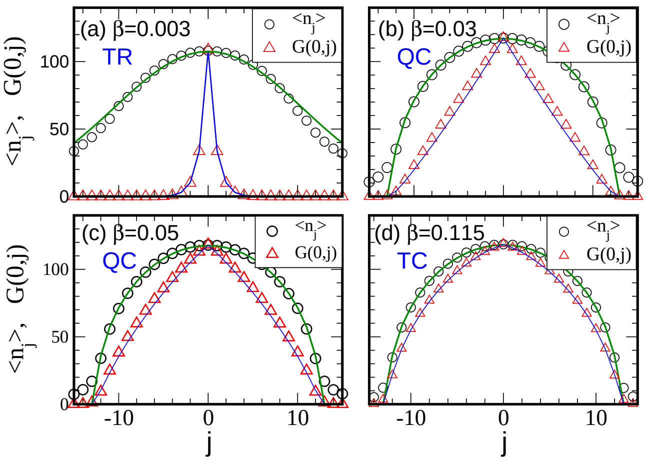

FIG. 3: (Color online) $N = 2000$, $U = 0.4$, $V_t = 0.3$. The density profiles $\sqrt{n_0 n_j}$ ($\circ$) are virtually independent of temperature for $\beta \geq \beta_{\rm QC} \approx 0.03$ (b)-(d), while the Green's function $G(0,j)$ ($\triangle$) varies with β. The lines are the analytical estimates, a Gaussian fit for $\sqrt{n_0 n_j}$ in (a), a TF profile $n_0\sqrt{1 - j^2/L^2}$ for $\sqrt{n_0 n_j}$ in (b)-(d) and $\sqrt{n_0 n_j}\exp(-\alpha|\ln[(L-j)/(L+j)]|)$ [see Eq. (2)] for $G(0,j)$.

no longer fluctuates: the density profiles n_j at different temperatures $\beta \geq \beta_{\rm QC}$ are identical and in excellent agreement with a TF inverse parabola shape of half size L, where L equals to $L_{\rm TF}$ [Figs. 2(b)- 2(d)]. However, thermal fluctuations of the phase are considerable. Thus, the width of the momentum profile, and the phase correlation function still change with decreasing temperature (Fig. 1). Figures 3(b)- 3(d) demonstrate that the Green's function varies substantially for different $\beta \geq \beta_{\rm QC}$, while the density profile $\sqrt{n_0 n_j}$ is invariant. We find very good agreement with the mean-field result Eq. (2): the ansatz $\sqrt{n_0 n_j}\exp\{-\alpha|\ln[(L-j)/(L+j)]|\}$, with α a fitting parameter, reproduces $G(0,j)$ (Fig. 3).

At temperatures much lower than $1/\beta_{\rm QC}$, phase fluctuations also become suppressed. Therefore, it is meaningful to introduce a second crossover temperature, $1/\beta_{\rm TC}$, to a phase-coherent regime, the true condensate. We define $\beta_{\rm TC}$ as the temperature where $C(0, 0.8L) = \exp(-0.25)$. This definition is somewhat arbitrary, but yields a scale below which the system can safely be considered to be phase-coherent. In addition, it allows for a comparison of analytical and numerical results, with the analytical equivalent of $\beta_{\rm TC}$ being $\tilde{\beta}_{\rm TC} = 4\beta_d \mu_{\rm TF}\ln(9)/3\hbar\omega$ [which is the temperature where $\langle \delta\hat{\phi}^2_{0z'}\rangle = 0.5$ for $|z'| = 0.8L_{\rm TF}$; see Eq. 2]. Note that the true condensate is not to be confused with a BEC, and strictly only appears at zero temperature (Thomas-Fermi condensate; see [10]). In the true condensate, the Green's function and the momentum profile approach their temperature-independent ground state shapes, as shown by the convergence of

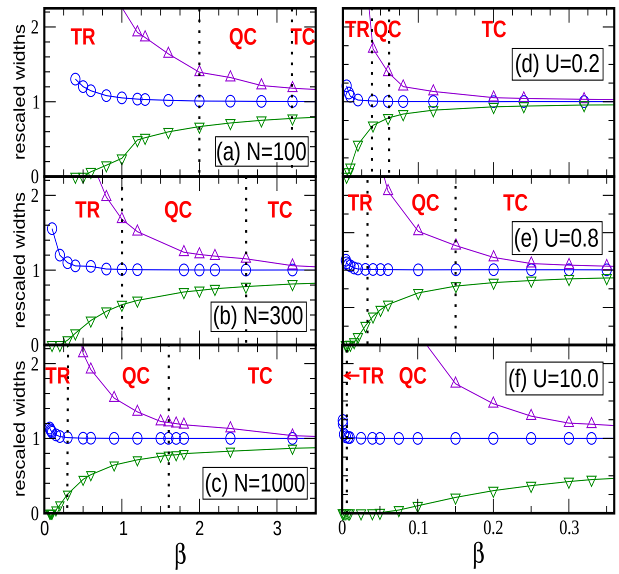

FIG. 4: (Color online) The size $s = \beta_{\rm TC}/\beta_{\rm QC}$, of the QC regime depending on the number of particles N (a - c, $U = 0.5$, $V_t = 0.01$) and coupling constant U (d - f, $N = 2000$, $V_t = 0.4$).
$L_n/L_n^{\rm sat}$ ($\circ$), $L_k/L_k^{\rm sat}$ ($\triangle$), $C(0, 0.8L)$ ($\bigtriangledown$)
a) $\gamma = 0.08$, $\tilde{\beta}_{\rm TC} = 3.5$, $\beta_{\rm TC} \approx 3.2(4)$, $\beta_{\rm QC} \approx 2.0$, $s \approx 1.6$
b) $\gamma = 0.04$, $\tilde{\beta}_{\rm TC} = 2.5$, $\beta_{\rm TC} \approx 2.6(4)$, $\beta_{\rm QC} \approx 1.0$, $s \approx 2.6$
c) $\gamma = 0.02$, $\tilde{\beta}_{\rm TC} = 1.64$, $\beta_{\rm TC} \approx 1.6(1)$, $\beta_{\rm QC} \approx 0.3$, $s \approx 5.3$
d) $\gamma = 0.001$, $\tilde{\beta}_{\rm TC} = 0.06$, $\beta_{\rm TC} \approx 0.06(2)$, $\beta_{\rm QC} \approx 0.04$, $s \approx 1.5$
e) $\gamma = 0.006$, $\tilde{\beta}_{\rm TC} = 0.15$, $\beta_{\rm TC} \approx 0.15(5)$, $\beta_{\rm QC} \approx 0.03$, $s \approx 5$
f) $\gamma = 0.17$, $\tilde{\beta}_{\rm TC} = 0.82$, NO $\beta_{\rm TC}$, $\beta_{\rm QC} \approx 0.01$, $s \approx \beta_{\rm QC}^{-1} = 100$
Comparison of (a)-(c), and (d)-(f), respectively, shows that s increases with increasing N and U.

$L_k(\beta)$ and $C(0, 0.8L)$ in Fig. 1. The system becomes practically phase coherencent, as illustrated in Fig. 3(d), where $\sqrt{n_0 n_j} \approx G(0,j)$. For the parameter set in Figs. 1-3, we find that $\beta_{\rm TC} \approx 0.115(5)$ which agrees with the analytical estimate $\tilde{\beta}_{\rm TC} = [(U^2/6NV_t^2)^{1/3}\ln(9)] = 0.116$.

We now study the appearance of a phase-fluctuating condensate depending on the system parameters U, V_t, and N. The WI limit is characterized by $\gamma = U/2n \ll 1$. We define the average density by $n = N/2L$. Since we find that L equals $L_{\rm TF}$ within error bars in all cases, we use $\gamma = (3U^4/4V_t N^2)^{1/3}$. Note that the magnitude of γ in the inhomogenous system differs from that in the homogeneous system. In Figs. 4(a)- 4(c), we demonstrate the effect of varying the number of particles N at on-site repulsion $U = 0.5$ and trapping $V_t = 0.01$. Both $\beta_{\rm QC}$ and $\beta_{\rm TC}$ decrease with increasing N, but since the change of $\beta_{\rm QC}$ is much greater than that of $\beta_{\rm TC}$, the region of the phase-fluctuating condensate, $s = \beta_{\rm TC}/\beta_{\rm QC}$, increases with increasing N. The effect of varying U is illustrated in Figs. 4(d)- 4(f), where $N = 2000$ and $V_t = 0.4$. Increasing U, causes $\beta_{\rm QC}$ to decrease, while $\beta_{\rm TC}$ increases. Thus $\beta_{\rm TC}/\beta_{\rm QC}$ grows with increasing U. More generally, the deeper we are in the Thomas-Fermi limit of large

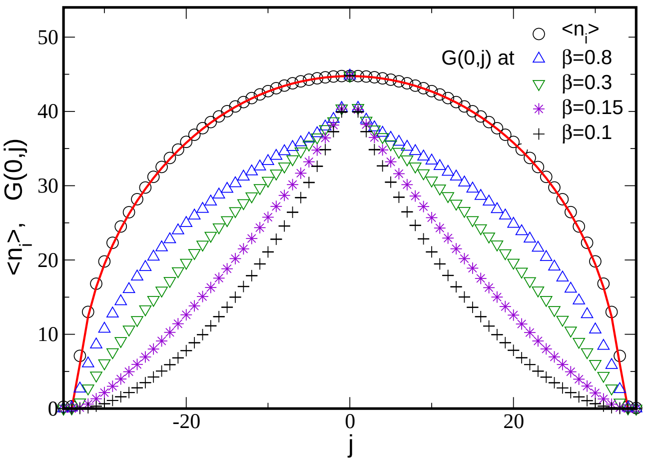

FIG. 5: (Color online) $N = 2000$, $U = 10.0$, $V_t = 0.4$ ($\gamma = 0.17$). The density profile $\sqrt{n_0 n_j}$ ($\circ$) is invariant for $\beta \geq \beta_{\rm QC} \approx 0.1$, while the Green's function $G(0,j)$ varies throughout the QC regime. However, $G(0,j)$ does not approach $\sqrt{n_0 n_j}$ (as in Fig. 3). The line is a TF fit to $\sqrt{n_0 n_j}$ with $L = 33.3$ ($L_{\rm TF} = 33.5$).

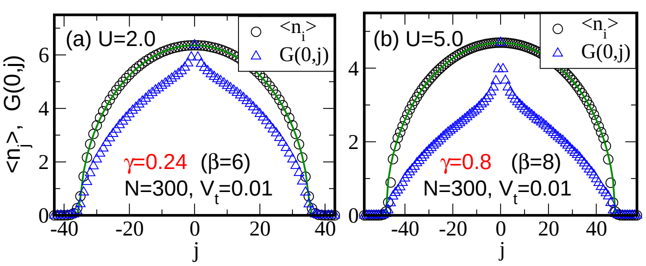

FIG. 6: (Color online) Ground state $\sqrt{n_0 n_j}$ ($\circ$) and $G(0,j)$ ($\triangle$) for different γ. The lines are fits to a TF profile with (a) $L = 35.2$ ($L_{\rm TF} = 35.6$) and (b) $L = 48.0$ ($L_{\rm TF} = 48.3$). For increasing γ, the correlation hole becomes more pronounced, and thus the quantum depletion increases.

$\mu_{\rm TF}/\hbar\omega \sim [(NU)^4/V_t]^{1/6}$, the larger is the size of the quasicondensate.

While for the parameter sets in Figs. 4(a)- 4(e), good agreement of $G(0,j)$ with expression (2) is observed for all β, as well as $\beta_{\rm TC} \approx \tilde{\beta}_{\rm TC}$, this does not apply to the example in Fig. 4(f), where $\gamma = 0.17$. Instead, $G(0,j)$ exhibits a qualitatively different behavior when approaching the ground state, as can be seen in Fig. 5: the phase-fluctutating condensate is beautifully realized, however, $G(0,j)$ does not approach $\sqrt{n_0 n_j}$ for $T \to 0$, and cannot be described by Eq. (2).

We consider the effect of stronger interactions in the trapped system on the phase-correlation properties in more detail. In Fig. 6, we show the ground state profiles for $N = 300$, $V_t = 0.01$, $U = 2.0$ and $U = 5.0$, respectively. We observe the same qualitative behaviour of the saturated Green's function as in Fig. 5. Close to the center of the cloud, where the density is higher, the decay of $G(0,j)$ is exponential; however, it broadens toward the outer, more diluted regions of the cloud. By comparing Figs. 6(a) and 6(b), it can be seen that for larger γ, the correlation hole in the central region of the condensate is larger. Clearly, the quantum depletion for the parameter sets in Fig. 6 is much more significant than for systems in the WI limit, since the number of particles with zero momentum $N(k=0) = \sum_{j,j'} G(j,j')/M$ decreases if $G(j,j') < \sqrt{n_j n_{j'}}$. We also observe this behavior if the density is smaller than 1 everywhere in the trap, and therefore exclude the possibility that it is an effect of the optical lattice. The shape of $G(0,j)$ is consistent with the two limiting cases, i.e. exponential decay in the strong-coupling limit, and phase-coherence [i.e. Eq.(2)] in the weak-coupling limit.

We conclude with a summary of our main results. In the mean-field, weakly interacting and Thomas-Fermi limits, both true a Thomas-Fermi condensate and a phase-fluctuating condensate emerge. Phase correlation properties, manifest in the characteristic decay of the single-particle density matrix, agree with surprising precision with the mean-field theory in [10]. In an intermediate-coupling regime, a true condensate no longer appears. The regime of the phase-fluctuating condensate persists even longer, extending to $T = 0$. We observe a qualitatively different decay of the Green's function, which cannot be accounted for by mean-field studies.

We acknowledge helpful discussions with Y. Castin, G. Shlyapnikov and T. Esslinger. This work was supported by a CNRS PICS grant (G.G.B. and F.H.) and the Swiss National Science Foundation. The simulations were performed on the Hreidar Beowulf cluster at ETH Zurich.

[1] N.D. Mermin and H. Wagner, Phys. Rev. Lett. **22**, 1133 (1966).
[2] P.C. Hohenberg, Phys. Rev. **158**, 282 (1967).
[3] L.P. Pitaevskii and S. Stringari, J. Low. Temp. Phys. **85**, 377 (1991).
[4] J.W. Kane and L.P. Kadanoff, Phys. Rev. **155**, 80 (1967); J. Math. Phys. **6**, 1902 (1965).
[5] F.D.M. Haldane, Phys. Rev. Lett. **47**, 1840 (1981).
[6] L. Reatto and G.V. Chester, Phys. Rev. **155**. 88 (1967).
[7] M. Schwartz, Phys. Rev. B **15**, 1399 (1977).
[8] W. Ketterle and N.J. van Druten, Phys. Rev. A **54**, 656 (1996).
[9] D.S. Petrov, M. Holzmann, and G.V. Shlyapnikov, Phys. Rev. Lett. **84**, 2551 (2000); D.S. Petrov, G.V. Shlyapnikov, and J.T.M. Walraven, *ibid.* **87**, 050404 (2001).
[10] D.S. Petrov, G.V. Shlyapnikov, and J.T.M. Walraven, Phys. Rev. Lett. **85**, 3745 (2000).
[11] I. Bouchoule, K.V. Kheruntsyan, and G.V. Shlyapnikov, Phys. Rev. A **75**, 031606(R) (2007).
[12] C. Mora and Y. Castin, Phys. Rev. A **67**, 053615 (2004).
[13] D.L. Luxat and A. Griffin, Phys. Rev. A **67**, 043603 (2003).
[14] N.M. Bogoliubov, C. Malyshev, R.K. Bullough and J.

Timonen, Phys. Rev. A **69**, 023619 (2004).

[15] Yu. Kagan, B.V. Svistunov, and G.V. Shlyapnikov, Sov. Phys. JETP **66**, 480 (1987); Yu. Kagan, V.A. Kashurnikov, A.V. Krasavin, N.V. Prokof'ev, B.V. Svistunov, Phys. Rev. A **61**, 043608 (2000).

[16] S. Dettmer *et. al.*, Phys. Rev. Lett. **87**, 160406 (2001); D. Hellweg *et. al.*, Appl. Phys. B: Lasers Opt. **73**, 781 (2001); S. Richard, F. Gerbier, J.H. Thywissen, M. Hugbart, P. Bouyer, and A. Aspect, *ibid.* **91**, 010405 (2003); J. Esteve, J.B. Trebbia, T. Schumm, A. Aspect, C.I. Westbrook, and O. Bouchoule, *ibid.* **96**, 130403 (2006); M. Hugbart *et. al.*, Europ. Phys. Jour. D **35**, 155 (2005).

[17] E.H. Lieb and W. Liniger, Phys. Rev. **130**, 1605 (1963); E.H. Lieb, Phys. Rev. **130**, 1616 (1963).

[18] D. Jaksch, C. Bruder, J.I. Cirac, C.W. Gardiner , and P. Zoller, Phys. Rev. Lett. **81** (1998) 3108.

[19] F. Dafolvo, S. Giorgini, L.P. Pitaevskii, and S. Stringari, Rev. Mod. Phys. **71**, 463 (1999).

[20] S.M.A. Rombouts, K. van Houcke, and L. Pollet, Phys. Rev. Lett. **96**, 180603 (2006); K. van Houcke, S.M.A. Rombouts, and L. Pollet, Phys. Rev. E **73**, 056703 (2006).